JPn Neuroscience
The Journal of Physiology

Crosslinking the ligand-binding domain dimer interface locks kainate receptors out of the main open state

Bryan A. Daniels, Elizabeth D. Andrews, Mark R. P. Aurousseau, Michael V. Accardi and Derek Bowie

Department of Pharmacology and Therapeutics, McGill University, Montréal, Québec, Canada

Key points

- This study identifies the gating structure responsible for controlling ion-channel sub-conductance behaviour at a major neurotransmitter receptor, namely kainate-type ionotropic glutamate receptor.
- Evidence is provided that the activation process may be made up of two clearly distinct conductance phases.
- The study speculates that functional diversity amongst ionotropic glutamate receptors emerged during evolution by re-deploying the same structures to carry out different tasks.

Abstract Kainate-selective ionotropic glutamate receptors (iGluRs) fulfil key roles in the CNS, making them the subject of detailed structural and functional analyses. Although they are known to gate a channel pore with high and low ion-permeation rates, it is still not clear how switches between these gating modes are achieved at the structural level. Here, we uncover an unexpected role for the ligand-binding domain (LBD) dimer assembly in this process. Covalent crosslinking of the dimer interface keeps kainate receptors out of the main open state but permits access to lower conductance states suggesting that significant rearrangements of the dimer interface are required for the receptor to achieve full activation. These observations differ from NMDA-selective iGluRs where constraining dimer movement reduces open-channel probability. In contrast, our data show that restricting movement of the dimer interface interferes with conformational changes that underlie both activation and desensitization. Working within the limits of a common architectural design, we propose functionally diverse iGluR families were able to emerge during evolution by re-deploying existing gating structures to fulfil different tasks.

(Received 20 February 2013; accepted after revision 23 May 2013; first published online 27 May 2013)
Corresponding author D. Bowie: Department of Pharmacology and Therapeutics, Bellini Building, Room 164, McGill University, 3649 Promenade Sir William Osler, Montreal, Québec, Canada H3G 0B1. Email: derek.bowie@mcgill.ca

Abbreviations AMPAR, AMPA-type ionotropic glutamate receptor; CNG, cyclic nucleotide gated; iGluR, ionotropic glutamate receptor; KA, kainate; KAR, kainate-type ionotropic glutamate receptor; LBD, ligand-binding domain; L-Glu, L-glutamate.

Introduction

Many neurotransmitter-gated ion channels in the mammalian CNS respond to agonist binding by opening to conductance states of different amplitudes (e.g. Hamill *et al.* 1983; Ascher *et al.* 1988; Mulle *et al.* 1991). Despite their prevalence in biology, the precise role fulfilled by sub-conductance levels in the signalling of neurotransmitter receptors is still not known. From a structural perspective, the occurrence of sublevels has often been explained by local electrostatic changes within the pore region itself (Fox, 1987; Barry *et al.* 1999). For example, cyclic nucleotide gated (CNG) channels (Root & MacKinnon, 1993) and vanilloid receptors (Liu *et al.* 2009), which are involved in sensory transduction of light and detection of noxious heat respectively, cycle through several sub-conductance states as a direct result of permeating protons binding to the pore. However, a number of reasons suggest that the multiple open states triggered

B. A. Daniels and E. D. Andrews contributed equally to this work.

DOI: 10.1113/jphysiol.2013.253666

by ionotropic glutamate receptor (iGluR) activation are regulated by structures that lie well outside the vicinity of the ion-conduction pathway.

Direct evidence linking long-distance allosteric events to subconductance states is best exemplified by the behaviour of AMPA-type iGluRs (AMPARs). Here, the unitary conductance has been shown to be directly linked to the number of agonist molecules bound to the receptor (Rosenmund *et al.* 1998; Smith & Howe, 2000) much like the behaviour of CNG channels (Ruiz & Karpen, 1997). At saturating agonist concentrations, the vast majority of AMPAR channels reside in the largest open state whereas smaller sublevels are encountered as the receptor's fractional occupancy decreases (Smith & Howe, 2000). How this mechanism provides added signalling flexibility, if any, to central glutamatergic synapses remains to be established; though it may play a role when vesicular neurotransmitter concentrations are thought to vary (McAllister & Stevens, 2000). Despite their close structural homology to AMPARs, kainate-type iGluRs (KARs) are not thought to be behave in this manner (Smith & Howe, 2000; but see Bowie & Lange, 2002; Swanson *et al.* 2002) suggesting that another set of rules may apply to this important iGluR subfamily.

Here, we designed experiments to understand how the LBD dimer interface controls KAR responsiveness. Covalent crosslinking of the KAR dimer interface via intermolecular disulfide bonds had a profound effect on the main conductance state. Specifically, KARs are locked out of the main open state but access a subset of conductance levels of lower amplitude. Interestingly, cross-linked KARs may still be able to desensitize because they appear to spend much of their time in long-lived shut states. Together, our data identify the LBD dimer interface as a key structural element that controls KAR responsiveness by switching the channel pore between high and low ion-permeation rates.

Methods

Cell culture and transfection

For electrophysiological experiments tsA201 cells were either transiently co-transfected with cDNA encoding wild-type or mutant GluK2(Q) and enhanced green fluorescent protein ($eGFP_{S65T}$) (Bowie, 2002) or transfected with cDNA encoding GluK2(Q) subunits with an internal ribosome entry site (IRES) upstream of mCherry. Y521C, L783C and Y521C/L783C GluK2 mutants were generated by site-directed mutagenesis. Residue numbering is of the full-length polypeptide (subtract 31 for GluK2 to obtain the predicted mature form). Cells were maintained in MEM containing 10% FBS (Invitrogen, Life Technologies Inc, Burlington, ON CAN) under a humidified atmosphere of 5% CO_2. Transfection was achieved using the calcium phosphate precipitation method. Electrophysiological recordings were performed 24–48 h after transfection.

Electrophysiological recordings

All recordings were performed at ∼22°C using an Axopatch 200B amplifier (Axon Instruments Inc., Foster City, CA, USA). Current records were filtered at 5 kHz for macroscopic responses and digitized at 25–50 kHz. Discrete single-channel currents were all acquired at 100 kHz, filtered by an 8-pole Bessel filter at 10 kHz and digitally filtered offline at 1–3 kHz. The reference electrode was connected to the bath via an agar bridge of 3 M KCl. Data were acquired using pClamp9 software (Axon Instruments Inc.), Spike 7.0 or Signal 5.0, Cambridge Electronic Design (CED) Limited, Cambridge England, and illustrated using Origin 7 (OriginLab Corp., Northampton, MA, USA) and Adobe Illustrator CS5 (Adobe Systems Inc., San Jose, CA, USA). External solutions contained (in mM): 150 NaCl, 5 Hepes, 0.1 $CaCl_2$, 0.1 $MgCl_2$, 2% Phenol Rred. The osmotic pressure was set to 290–300 mosmol l^{-1} using sucrose and the pH adjusted to 7.35 with NaOH. The internal solution contained (mM): 115 NaCl, 10 NaF, 5 Hepes, 5 Na_4BAPTA, 0.5 $CaCl_2$, 1 $MgCl_2$, and 10 Na_2ATP to chelate endogenous polyamines. pH and osmotic pressure were adjusted to match external solutions. Agonist solutions were prepared by dissolving the agonist in external solution and adjusting the pH appropriately.

Experiments were performed on excised membrane patches in the outside-out configuration for experiments examining macroscopic and microscopic GluK2 responses (Figs 1, 3 and 4) and the inside-out configuration for measurement of single-channel events (Figs 5–7). Thin-walled borosilicate glass pipettes (2–6 MΩ, King Precision Glass, Inc. Claremont, CA, USA) coated with dental wax were used for macroscopic experiments. To obtain low noise single-channel recordings, the tips of thick-walled borosilicate (16–30 MΩ, Harvard Apparatus Ltd., Holliston, MA, USA) or quartz (5–10 MΩ, King Precision Glass, Inc) electrodes were coated with Sylgard (Dow Corning, Midland, MI, USA). Agonist solutions were rapidly applied to outside-out patches for 250 ms at −60 mV, unless otherwise noted, using a piezo-stack driven perfusion system. Sufficient time between applications of glutamate was allowed for complete recovery from macroscopic desensitization. Solution exchange time was determined routinely at the end of each experiment by measuring the liquid junction current (10–90% rise-time = 100–400 μs). For inside-out patch experiments, 10 mM L-glutamate (L-Glu) or 1 mM kainate (KA) was applied to the pipette solution and the holding voltage set to −100 mV. Recordings obtained had a baseline root mean squared (RMS) noise recorded from

the amplifier of 0.2–0.4 pA while the headstage was set to the capacitive feedback recording mode.

Stationary noise analysis

For stationary noise analysis (Neher & Stevens, 1977) data were filtered and acquired as above for macroscopic responses. For individual patches at least 30 s of recording was obtained at −30 mV in control solution before moving to 50 μM, 500 μM or 10 mM glutamate for 10–30 s. Each n value is represented by the average weighted unitary conductance of 2–4 responses from a single patch. Data were compressed by a factor of 5 and bandpass filtered (between 1 and 1000 Hz) in Channel Lab (Synaptosoft, Decatur, GA, USA). Power spectra (4096 spectral points) were generated from the baseline and response regions of the resulting trace and the difference of these spectra was fitted with a sum of two Lorentzian components:

$$G(f) = \{G(0)_1/[1+(f/f_{c1})^2]\} + \{G(0)_2/[1+(f/f_{c2})^2]\},$$

where $G(f)$ is the net one-sided spectral density, f is the frequency, $G(0)_1$ and $G(0)_2$ are the zero-frequency asymptotes and f_{c1} and f_{c2} the corner frequencies. Current variance, $\sigma^2(I)$, was calculated from the Lorentzian fit as, $\sigma^2(I) = \pi/2(G(0)_1 f_{c1} + G(0)_2 f_{c2})$. Given that the variance increased in a linear manner with increasing agonist concentration (50 μM–10 mM L-Glu), we concluded that the apparent open channel probability was low. Therefore, the apparent single-channel current (i) was calculated as, $i = \sigma^2/I$, where I is the individual mean steady-state glutamate current and the weighted unitary conductance (γ) was calculated as, $\gamma = i/(V_m - V_{rev})$, from the known holding potential ($V_m = -30$ mV) and assumed reversal potential ($V_{rev} = 0$ mV).

Single-channel analysis

Digitally filtered data were exported to Signal 5.0 (CED) to perform time course fitting using SCAN (Colquhoun & Sigworth, 1995). The idealized records were then used to provide information on shut times, open times and response amplitudes. Working with a cut-off frequency (f_c) of 1 kHz, transitions briefer than 2 times the filter rise-time (t_r) (i.e. 98% of full amplitude) were excluded from the analysis of amplitudes (0.7 ms). Patches chosen for analysis had an averaged 1 kHz filtered RMS of 0.077 pA for wild-type GluK2, and 0.047 pA for mutant GluK2. Apparent transitions that were greater than 2 × RMS between open and closed states were fitted. In the resulting idealized records, a safe minimum resolvable duration of 0.9 ms for openings and 0.8 ms for shuttings was imposed. A false event rate (λ_f) of less than 2% of the true event rate was obtained using the equation $\lambda_f = f_c \times \exp(-\varphi^2/2\sigma_n^2)$, where φ = lowest sublevel amplitude and σ_n = baseline noise. Origin 7.0 was used for the analysis of amplitude distributions, and the Gaussian function was used to find peak amplitudes, $y = [A/w \times \mathrm{sqrt}(\pi/2)] \times \exp[-2 \times (x-xc)/w]^2$, where A = area, xc = centre of the peak, w = error associated with xc. Channel lab (Synaptosoft Inc.) was used to fit open and shut times with the sum of three or four exponentials using the maximum likelihood method. The number of Gaussian and/or exponential components was determined by fitting the combined data shown in Figs 5–7 by eye. This was verified by ensuring that the same number of components was consistently needed to fit data from individual patch recordings (Colquhoun, 1994).

Results

Crosslinking the dimer interface disrupts kainate receptor functionality

The stability of the dimer interface of both AMPARs and KARs is thought to regulate the onset of receptor desensitization. This is supported by two lines of functional evidence at AMPARs. First, allosteric modulators such as cyclothiazide and aniracetam bind to the dimer interface (Sun *et al.* 2002; Jin *et al.* 2005) and delay the onset of macroscopic (Partin *et al.* 1996) and microscopic desensitization (Rosenmund *et al.* 1998). Secondly, restricting dimer interface movement by mutation of key amino acid residues generates AMPARs with non-decaying macroscopic response profiles (Stern-Bach *et al.* 1998; Weston *et al.* 2006). Although KAR desensitization cannot be blocked by allosteric modulators, crosslinking or mutation of the dimer interface, like the Y521C/L783C GluK2 KAR (Fig. 1) (equivalent to Y490C/L752C in Weston *et al.* 2006), also gives macroscopic responses that show little sign of decay in the continued presence of the agonist (Priel *et al.* 2006; Weston *et al.* 2006; Nayeem *et al.* 2009; Chaudhry *et al.* 2009).

To investigate the possible role of the LBD dimer interface in determining KAR responsiveness, we studied the Y521C/L783C GluK2 mutant where cysteine residues were introduced to stabilize the dimer interface (Fig. 1*A* and *B*). For comparison, we also expressed GluK2 receptors with single cysteine mutations at position Y521 or L783 (Fig. 1*B*). In our initial electrophysiological analysis, we noticed that the averaged maximum response elicited by 10 mM L-Glu acting on the GluK2 double mutant (85 ± 18 pA, $n = 13$) was more than an order of magnitude smaller than the averaged peak response at wild-type GluK2 receptors (2.3 ± 0.6 nA, $n = 16$). Peak L-Glu responses obtained from GluK2 Y521C were similar to the wild-type receptor (726 ± 144 pA, $n = 4$) whereas the L783C mutant yielded no discernible current ($n = 10$).

Our finding with the Y521C/L783C GluK2 receptor was surprising since the KAR response should be equal or larger if desensitization is absent, as is the case when GluA1 AMPAR is treated with cyclothiazide (Partin *et al.* 1996). A possible explanation for this difference is that crosslinking the dimer interface disrupts GluK2 receptor surface expression as suggested for another GluK2 double-cysteine dimer mutant, K696C/E787C (Priel *et al.* 2006). However, it is also possible that crosslinking the KAR dimer interface affects the gating properties of the receptor, such as single-channel conductance or open-channel probability. To examine this possibility, we made direct comparisons of the single-channel events elicited by rapid application of L-Glu onto wild-type and mutant GluK2 receptors.

Crosslinking the dimer interface keeps GluK2 receptors out of the main open state

Data summarizing experiments of agonist-evoked single-channel events in outside-out patches are shown in Fig. 2. Following rapid application of 10 mM L-Glu (400 ms duration, $V_H = -60$ mV), wild-type GluK2 receptors rapidly enter into several open states up to 30 pS in amplitude (Fig. 2*A*) as noted by others (Zhang *et al.* 2009). Since we have not restricted our study to patches containing a single GluK2 channel, we have not systematically documented the distribution of single-channel amplitudes which would be distorted by the near simultaneous opening of multiple channels (Aldrich *et al.* 1983). However, visual inspection of the data by overlaying multiple sweeps from the same recording revealed that the largest open state was close to 30 pS (Fig. 3*A*) which agrees with prior work (Zhang *et al.* 2009). As expected, channel activity in all our recordings occurred shortly after agonist application returning to baseline within 20–30 ms (Fig. 2*A*). Cessation of channel activity can be explained by the onset of GluK2 receptor desensitization, which is a prominent feature of these receptors (Bowie & Lange, 2002). In support of this, averaging many sweeps obtained from an individual patch recording generated an ensemble response (Fig. 2*C*) that was similar to the rapidly rising, decaying macroscopic response routinely observed in patches of hundreds to thousands of channels (Bowie & Lange, 2002). For example, the averaged decay time constant from six patches (peak, 2.3 ± 0.7 pA) where discrete channel openings were observed was 4.2 ± 0.6 ms, which was similar to the 5.7 ± 0.3 ms of patches containing many more channels (peak 2.3 ± 0.6 nA, $n = 16$).

The rapid inactivating behaviour of wild-type GluK2 receptors also provides insight into how KARs would behave if desensitization was abolished. In the absence of desensitization, KAR channel activity would be expected not to 'switch off' but instead remain in the main open state of 30 pS as long as the agonist is present. This prediction is in keeping with the single channel behaviour of non-desensitizing AMPA receptors (Rosenmund *et al.* 1998; Smith & Howe, 2000) and the outcome of numerical simulations of any of the GluK2 receptor gating models (Heckmann *et al.* 1996; Bowie *et al.* 1998; Barberis *et al.* 2008) that have only had their desensitized states removed. To illustrate this latter point, simulations of single-channel events were compared using a previously published gating model of GluK2 receptors (Bowie *et al.* 1998). As expected, channel activity quickly declines with saturating agonist concentrations using this model of wild-type GluK2 receptors where desensitization is intact (Fig. 3*C*). In contrast, single GluK2 receptors reside almost continuously in the main open state when desensitized states are removed (Fig. 3*D*) establishing a general principle that should also be observed with Y521C/L783C GluK2 receptors.

Despite this prediction, we had difficulty clearly resolving single-channel events from Y521C/L783C GluK2 receptors. This was particularly true for recordings at a holding potential of −60 mV. However, at the more

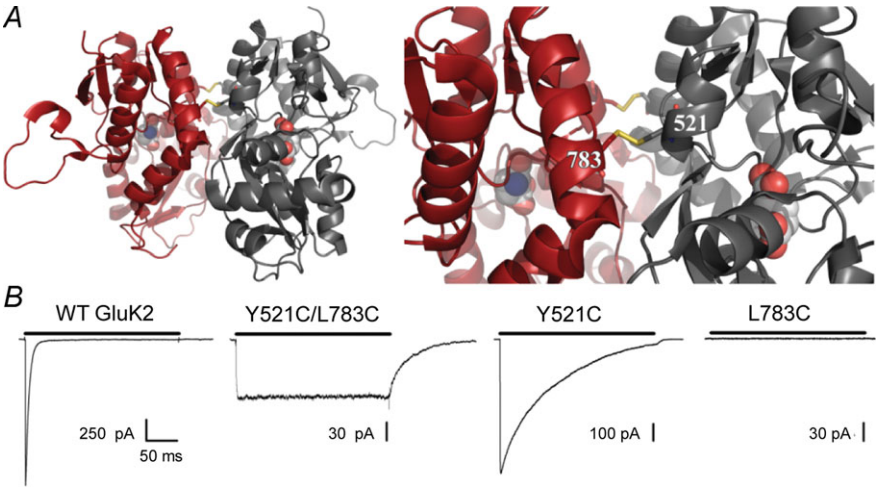

Figure 1. Crosslinking the LBD dimer assembly affects KAR functionality
A, crystal structure of the Y521C/L783C ligand-binding domain in complex with L-Glu (PDB 2IOC, Weston *et al.* 2006). Two different views of the dimer interface showing the introduced disulfide bonds (shown in yellow) between cysteine residues from adjacent GluK2 subunits. *B*, peak responses to 10 mM L-Glu application on outside-out patches expressing wild-type (WT) (patch 091116p4), Y521C/L783C (patch 09111p24), Y521C (patch 120220p11) and L783C (patch 120503p3) (250 ms agonist pulse, holding potential (V_H) equals −60 mV).

hyperpolarized potential of −100 mV, we could observe brief and small amplitude single-channel activity (Fig. 2*B*). With the increased driving force, it was possible to observe marked differences between the behaviour of wild-type and mutant GluK2 receptors. The most notable distinction was the complete absence of measurable openings to the wild-type main conductance state of 30 pS. A direct comparison of several sweeps of Y521C/L783C GluK2 channel activity with that of wild-type receptors, both at a holding potential of −100 mV, is shown in Fig. 3*A* and *B*. We were surprised that such short-lived single events could give rise to macroscopic responses that decay little in the continued presence of the agonist (Fig. 1*B*). However, the ensemble response obtained from averaging many single-channel sweeps from the same patch recording closely matched this behaviour (Fig. 2*D*). In four patches the number of channels was low enough to clearly see discrete, albeit transient, events. The averaged ensemble currents from these patches had non-decaying responses (0.24 ± 0.09 pA) and upon agonist removal had a decay constant of 14.8 ± 2.9 ms that was similar to responses obtained from patches with much larger responses (85 ± 18 pA, 11.8 ± 0.6 ms, $n = 13$).

When taken together, these data demonstrate that covalent crosslinking of the LBD dimer interface of the GluK2 receptor does not block desensitization by locking KARs into the main open state. However, the double-cysteine mutation may block desensitization while simultaneously rendering glutamate a poor agonist due to the imposed movement constraints as has been implied at AMPARs (Weston *et al.* 2006). To accurately estimate the amplitude of individual Y521C/L783C GluK2 events from these recordings, we next determined their unitary conductance.

Double-cysteine mutant GluK2 receptors have a low weighted unitary conductance

To examine the effect of Y521C/L783C GluK2 on conductance, we estimated its weighted unitary conductance by stationary noise analysis and compared it to that of wild-type receptor (Fig. 4). To do this,

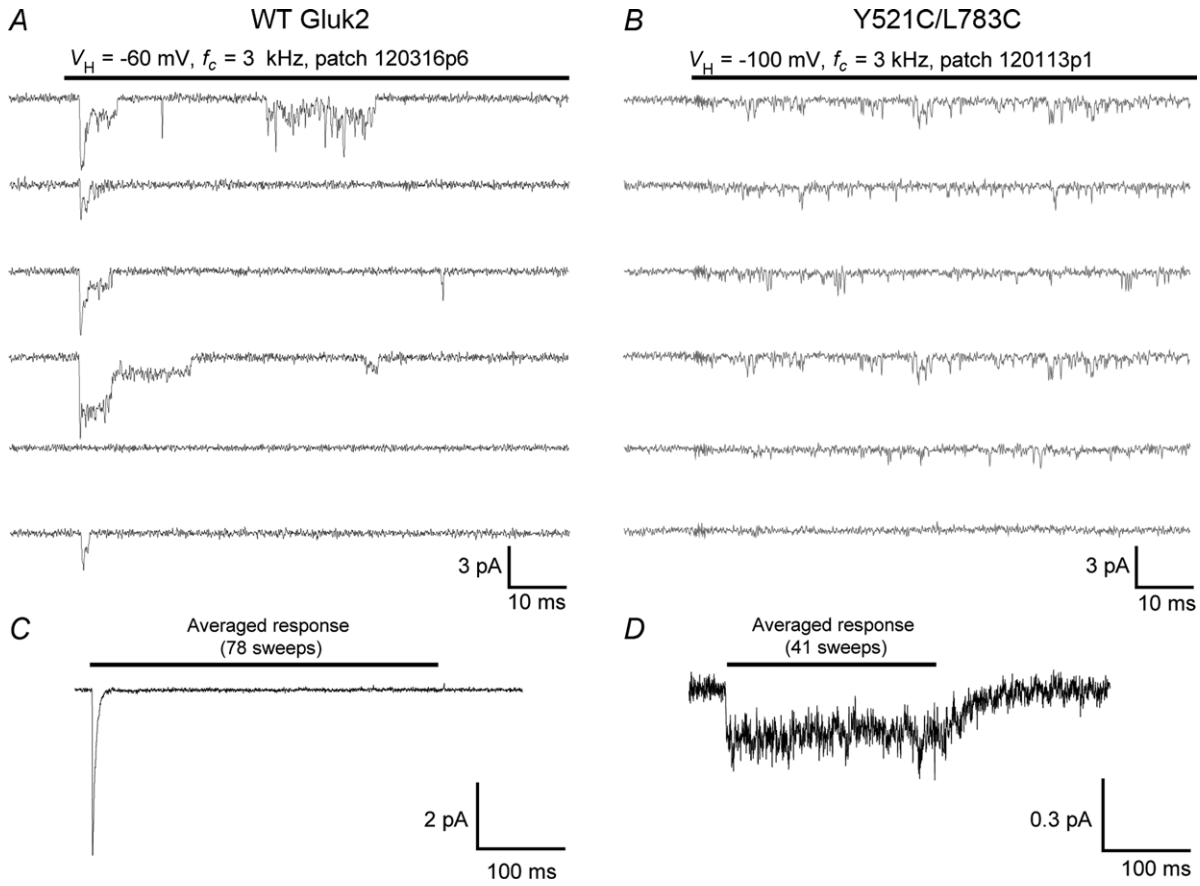

Figure 2. Y521C/L783C GluK2 receptors gate channels that are brief and small in amplitude
Example sweeps of two outside-out patches expressing few wild-type (WT; *A*) or Y521C/L783C GluK2 (*B*) receptors show discrete channel openings and closures in response to 10 mM L-Glu (filled bars). *C* and *D*, consecutive sweeps from the same patches produced averaged responses that were phenotypically identical to macroscopic responses. Offline filter frequency (f_c) and holding potential (V_H) are indicated.

baseline-subtracted membrane noise elicited by L-Glu (50 μM, 500 μM or 10 mM) acting on mutant or wild-type GluK2 receptors was fitted with the sum of two Lorentzian components (Fig. 4*A* and *B*). Using this approach, we estimated the chord conductance of Y521C/L783C GluK2 receptors to be 3.7 ± 0.3 pS ($n = 9$, Fig. 4*B* and *C*). By comparison, membrane noise elicited by wild-type GluK2 receptors gave a chord conductance of 6.9 ± 0.7 pS ($n = 9$, Fig. 3*A* and *C*) which was statistically different from the mutant receptor value ($P < 0.001$, Fig. 4*C*). Alternatively, we performed a linear regression on mean current-variance plots and obtained chord conductances of 3.2 pS (Y521C/L783C) and 5.2 pS (wild-type GluK2; Supplemental Fig S1).

Although our wild-type data are in good agreement with another noise analysis study (Swanson *et al.* 1996), it is nevertheless 4- to 5-fold lower than single-channel measurements of the main open state (Zhang *et al.* 2009). It is worth noting that stationary noise analysis is performed on data obtained at equilibrium whereas the large, main open state for GluK2 receptors (27 pS) has been observed under non-equilibrium conditions following rapid L-Glu applications (Zhang *et al.* 2009). Consequently, the apparent discrepancy between these two datasets may be explained if unitary conductance estimates are dependent on when the measurement takes place. In fact, this possibility is in keeping with prior work from our lab suggesting that peak and equilibrium GluK2 responses have distinct channel conductance (Bowie & Lange, 2002; Bowie *et al.* 2003; Maclean *et al.* 2011).

Activation of Y521C/L783C GluK2 receptors at equilibrium elicits low amplitude events

Discrete channel measurements observed in inside-out patches were conducted in the continuous presence of a saturating concentration of L-Glu (10 mM) to reproduce conditions of the outside-out patch experiments (i.e. Figs 2 and 3). Visual inspection of the records revealed that Y521C/L783C GluK2 receptors gate channels that sojourn to two distinct levels for brief periods of time (Fig. 5*A* and *B*). Given their small amplitude, we were initially concerned that many of the smallest transitions (i.e. 2.4 pS) corresponded to false events in our idealized records (Colquhoun & Sigworth, 1995). However, we concluded this was not the case since the estimates of

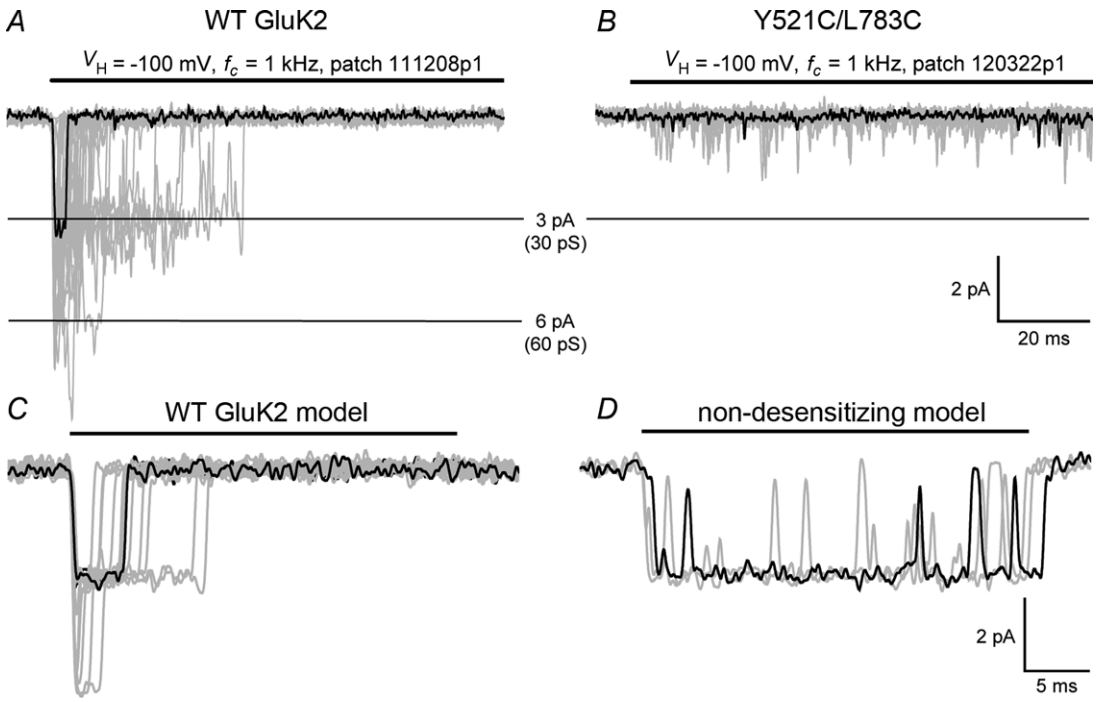

Figure 3. Y521C/L783C GluK2 receptors are locked out of the main open state
A comparison of glutamate-evoked channel openings from two different patches expressing minimal WT (*A*) and Y521C/L783C (*B*) GluK2 receptors. Consecutive sweeps (35–40 sweeps) were overlaid to demonstrate that wild-type openings are consistently measured at 30 and 60 pS before closing completely. Y521C/L783C displays brief sporadic openings of lower amplitude. Single sweeps are highlighted in black and the wild-type response is presumably the opening of one channel representing the WT GluK2 main open state. Offline filter frequency (f_c) and holding potential (V_H) are indicated. *C*, simulated responses to 10 mM L-Glu using the GluK2 receptor gating model described in Bowie *et al.* (1998). *D*, simulations of a single GluK2 channel using the same gating model but with the mono- and di-liganded desensitized states removed. Random noise was added to simulations in panels *C* and *D*.

the false event rate of the lowest sublevel amplitude was sufficiently low at 0.025 s^{-1}. Thus, in a typical recording of 10–20 min, the number of false events was about 15–30 which would not significantly impact the outcome of our analysis. More importantly, transitions between each open state could be directly observed in some records (Fig. 5*B*, see arrow), demonstrating that they indeed represent distinct open states of the same channel. Given this, the bin width chosen to fit amplitude distributions took into consideration the expectation of observing two distinct sublevels (Methods, Fig. 5*D*). Fits of the distributions showed that the majority of openings elicited by mutant GluK2 receptors exhibited a conductance of 2.4 pS (65%, Table 1), with a smaller proportion of 4 pS (35%). Importantly, both of these open states are about an order of magnitude smaller in amplitude than the largest wild-type GluK2 receptor open state (i.e. 27 pS) (Zhang *et al.* 2009). This finding reaffirms why excised macroscopic patches containing mutant receptors have smaller amplitudes (cf. Fig. 1). That is, the same number of mutant receptors on the plasma membrane would give smaller ensemble responses than wild-type receptors given their smaller unitary conductance.

In agreement with other studies, we observed that the vast majority of single-channel events elicited by wild-type GluK2 receptors, where desensitization is intact, also access open states of low amplitude (Fig. 5*C* and *E*). To generate amplitude distributions, data for wild-type GluK2 single-channel openings were analysed using the same bin width as mutant GluK2 data. Like mutant GluK2 receptors, most of the openings for wild-type receptors have conductances of 2.6 pS (33%) and 4 pS (40%), with fewer openings to 6 pS (14%), 8 pS (4%) and 10 pS (9%) (Fig. 5*E*, Table 1). A comparison of open times between wild-type and mutant GluK2 receptors also revealed that most events were brief in duration, lasting just a few milliseconds (i.e. mutant $\tau_{fast} = 4.7$ ms (83%) *vs.* wild-type $\tau_{fast} = 2.7$ ms (86%); Fig. 7). Given their amplitude, it is possible that the larger conductance states observed represent the simultaneous opening of several channels of lower conductance within a patch. However, we have concluded that this is probably not the case since we have observed direct transitions to these larger open states in our records regardless of the filter cut-off frequency (Fig. 6*A*). Consequently, we considered the possibility that these larger conductance states represent GluK2 receptors that have partially recovered from desensitization. If true, we reasoned that the occurrence of these larger open states would be less frequent in recordings of single events elicited by the agonist, kainate (KA), which favours GluK2 receptor desensitization for much longer periods of time (Fay *et al.* 2009). In agreement with this, 84% of all single-channel events observed in the continuous presence of 1 mM KA sojourn to conductance states of 2.7 pS (48%) or 4 pS (36%), with fewer to 6 pS (16%) (Fig. 6*B* and *C*). We did observe larger events (up to 20 pS) but

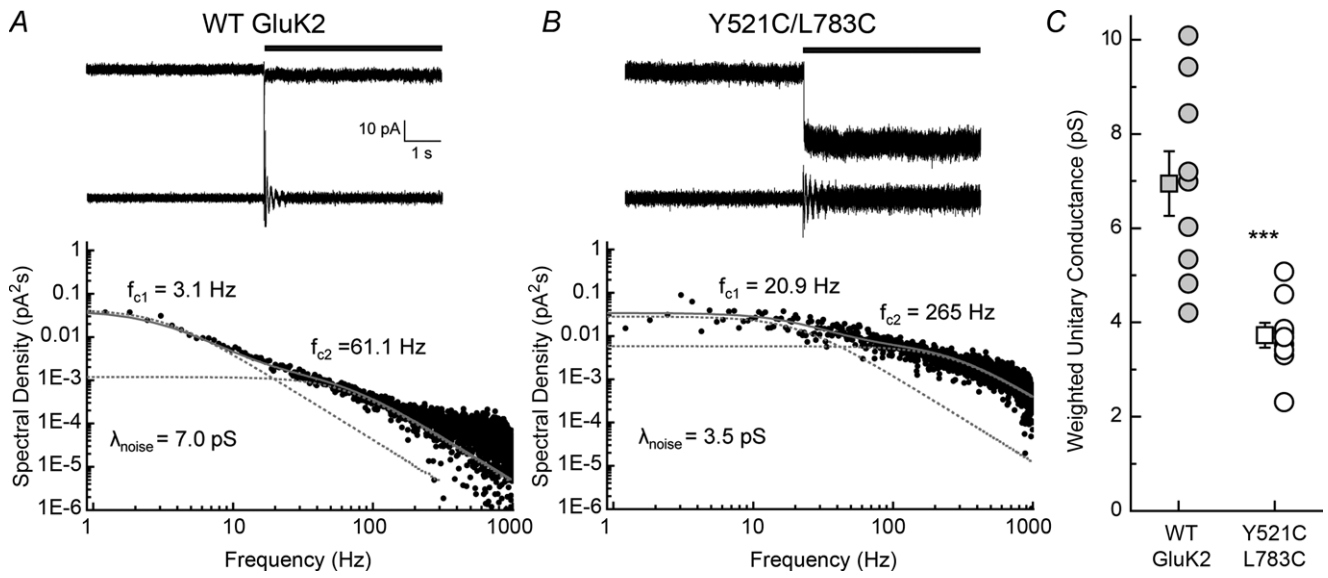

Figure 4. Stationary noise analysis shows that the Y521C/L783C KAR has a lower weighted unitary conductance than the wild-type (WT) GluK2 receptor
Representative traces of WT (*A*; patch 100112p2) and Y521C/L783C- (*B*; patch 10012p3) GluK2 receptors responding to 500 μM L-Glu (filled bars, $V_H = -30$ mV). Bandpass filtered traces (1 Hz to 1 kHz) are shown below the recorded traces. Power spectra were fitted with the sum of two Lorentzian functions (grey lines) and the resulting variance was used to calculate the weighted unitary conductance. Dotted lines indicate each single Lorentzian fit and half-power frequencies are indicated. *C*, scatter plots of individual and mean weighted unitary conductance determined by exposure to 50 μM, 500 μM or 10 mM glutamate. $^{***}P < 0.001$.

their occurrence was too infrequent to permit proper analysis. As with previous recordings using L-Glu, the false event rate with 1 mM KA was also low (i.e. 0.085 s^{-1}, 5 per minute).

We can make two general conclusions from these observations. First, crosslinking the dimer interface does not generate a GluK2 receptor with entirely new conductance states. Instead, we conclude that mutant

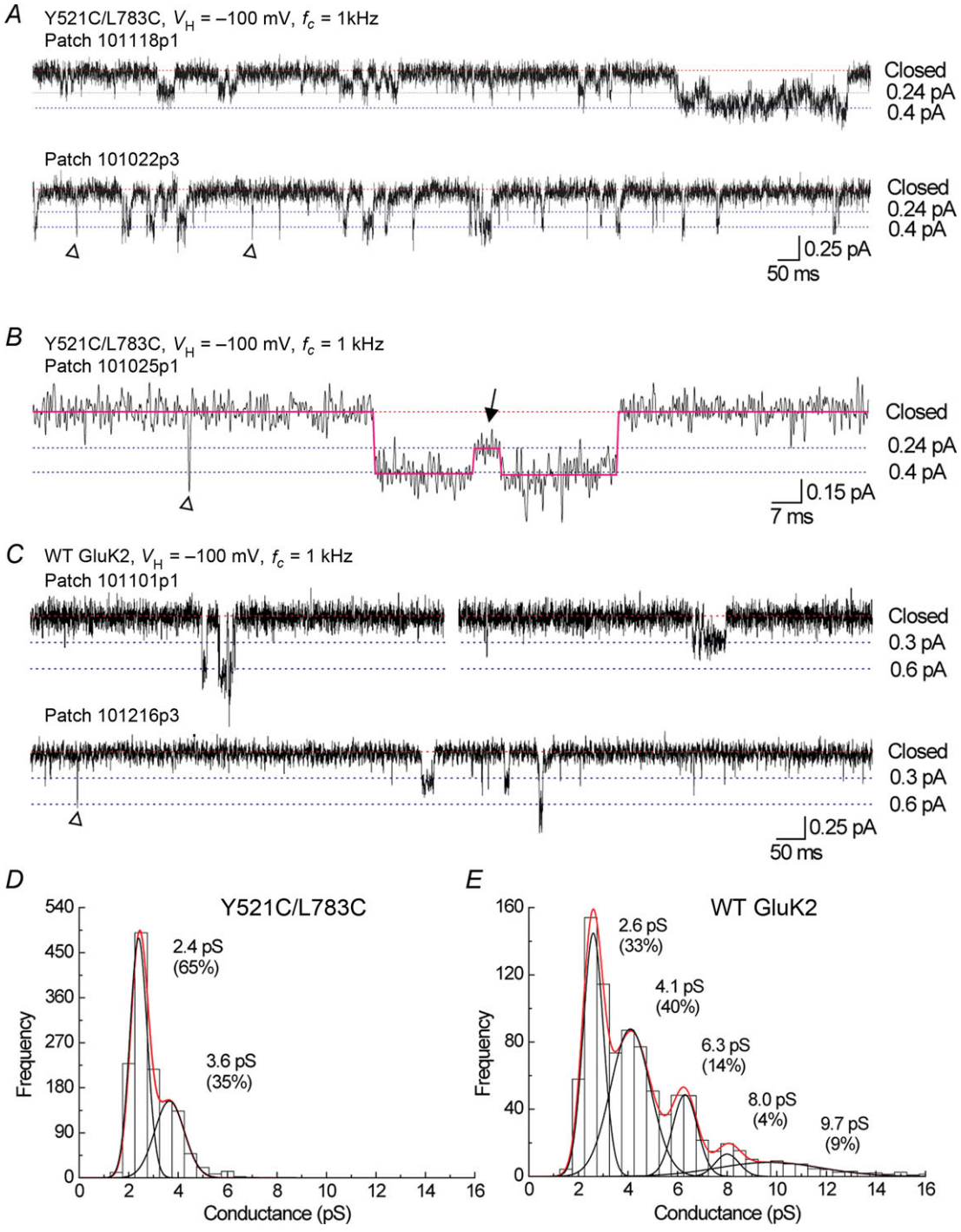

Figure 5. Crosslinking the dimer interface restricts KARs to low subconductance levels
Typical single-channel events recorded in 10 mM L-Glu at a holding potential (V_H) of −100 mV. Each trace corresponds to regions of high activity from inside-out patches expressing Y521C/L783C (*A* and *B*) and wild-type (WT) (*C*) GluK2 receptors. Arrowheads indicate transient events shorter than imposed time resolution. Frequency distributions of open conductances elicited from Y521C/L783C (*D*; $n = 4$) and WT GluK2 (*E*; $n = 4$) receptors were fitted with the sum of two and five Gaussian components, respectively.

Table 1. Single-channel properties of mutant and wild-type GluK2 in response to 10 mM L-Glu

	Subconductance levels	Event frequency	Open times	Event frequency	Shut times	Event frequency
Wild-type GluK2	2.6 pS	34%	2.7 ms	85%	4.2 ms	22%
($n = 4$ patches, 3098 events)	4 pS	39%	10.1 ms	13%	49 ms	16%
	6 pS	14%	76.3 ms	2%	484 ms	17%
	8 pS	4%			3.1 s	45%
	10 pS	9%				
Y521C/L783C GluK2	2.4 pS	65%	4.7 ms	83%	13 ms	14%
($n = 4$ patches, 5007 events)	4 pS	35%	17 ms	14%	129 ms	44%
			76 ms	3%	733 ms	32%
					3.6 s	10%

receptors can access only a subset of open states that would be normally available to the wild-type GluK2 receptor. Second, our observations are consistent with an earlier model of GluK2 receptor desensitization where open states of intermediate conductance represent partially desensitized KAR tetramers (Bowie & Lange, 2002).

Y521C/L783C GluK2 receptors cycle through long-lived shut states

Desensitization of ligand-gated ion channels is almost universal and broadly defined as a long-lived, agonist-bound closed or non-conducting state (Katz & Thesleff, 1957; Colquhoun & Ogden, 1988). Given this, we compared the time wild-type and mutant GluK2 receptors resided in long-lived shut states. Visual inspection of single-channel recordings from patches containing the double-cysteine mutant receptors already suggested that they spend time in a closed conformation(s) like wild-type receptors. In fact, in the continuous presence of saturating agonist, mutant GluK2 receptors spend only about 2% of their time (i.e. total open time/entire recording time; range = 0.4–4%, $n = 4$) in the open state, which is comparable to wild-type GluK2 receptors (0.6%, range = 0.1–1%, $n = 4$) under the same recording conditions. In keeping with this, fits of shut time distributions revealed that both receptor types have four distinct shut time components (Fig. 7*C* and *D*, Table 1). Wild-type GluK2 receptors had shut components of 4.2 ms (22% contribution), 49 ms (16%), 484 ms (17%) and 3.1 s (45%). Mutant GluK2 receptors had similar shut components of 13 ms (14%), 129 ms (44%), 733 ms (32%) and 3.6 s (10%), although weighted to more intermediate values. Importantly, fit values of shut time distributions are likely to be underestimated since it is probable that the activity of more than one channel is being detected in each of our recordings. Furthermore, in both wild-type and mutant recordings very brief events were not analysed (see arrowheads in Fig. 5) due to the time resolution imposed by the filter cut-off frequency (1 kHz). This frequency was necessary to accurately measure the small amplitudes of the double-cysteine GluK2 but would lead to an overestimation of the length of shut times for both mutant and wild-type GluK2 receptors. Taken together, the occurrence of long-lived shut states is consistent with the possibility that, although macroscopically non-decaying, crosslinked KARs are able to desensitize at the single-channel level.

Discussion

The present study advances our understanding of iGluRs in several substantial ways. First, we identify the stability of the KAR LBD dimer interface as a key regulator of subconductance behaviour. Given their close structural and functional similarity to AMPARs, it would be interesting to test if this other iGluR family is similarly controlled. Second, this study adds to an emerging view of KARs where separate structural events may constitute peak and steady-state agonist responses (see below). Transient activation is thought to be governed by closed-cleft stability of the agonist-binding pocket as proposed recently (Maclean *et al.* 2011) whereas data presented here suggest a link between dimer interface stability and steady-state KAR activation. Third and finally, these findings suggest that rearrangement of the dimer interface is essential for normal KAR activation and desensitization.

Dimer stability and kainate receptor desensitization

Evidence linking the onset of KAR desensitization to the stability of the dimer interface was based on two substantive but nevertheless correlative findings. The first line of evidence came from electrophysiological recordings which showed that engineered mutations within the dimer interface affect decay rates of macroscopic KAR responses (Fleck *et al.* 2003; Zhang *et al.* 2006; Chaudhry *et al.* 2009; Nayeem *et al.* 2009). Even more compelling were experiments showing that restricting dimer

interface movement by cross-linked cysteine residues generated KARs with an apparently 'non-desensitizing' phenotype (Priel *et al.* 2006; Weston *et al.* 2006). The second line of evidence was derived from biochemical data showing that many of the same engineered dimer mutations and crosslinking manipulations had predictable effects on dimer stability as ascertained by analytical ultracentrifugation (Weston *et al.* 2006; Nayeem *et al.* 2009; Chaudhry *et al.* 2009).

Though these results were compelling, three important issues have been either overlooked or not fully explained in previous studies. First, the occurrence of desensitization can only be truly confirmed by examining single-channel events. For example, Rosenmund and colleagues (Rosenmund *et al.* 1998) have shown that a single AMPAR lacking desensitization remains in the main open state as long as the agonist is present. KARs are expected to behave similarly. In support of this, numerical simulations with GluK2 receptor gating models predict that single channels would also be continuously activated by agonist when desensitized states are removed (see Fig. 3*D*). However, direct examination of the single channel properties of double-cysteine KARs reveals that they do not exhibit this behaviour (see Fig. 3*B*). Given this, if crosslinking the LBD dimer interface of GluK2 receptors genuinely removes desensitization, it must also affect other aspects of receptor function.

A second related issue is that the introduced cysteines may do more than simply crosslink the dimer interface. Although, we have confirmed by Western blot analysis that the introduced cysteines residues form disulfide bonds, dithiothreitol treatment to disrupt cross-linked receptors in excised patches did not convert the non-decaying phenotype of the mutant to that of the wild-type receptor (data not shown). This observation is contrary to the conclusions of Weston *et al.* (2006), but ongoing experiments from our lab suggest that an important consequence of introducing either single- or double-cysteine residues is to alter the electrostatic environment of LBD dimer interface which accounts for their unexpected functional behaviour.

The third issue relates to observations describing the behaviour of crosslinked AMPARs. Like KARs, the equivalent double-cysteine mutation in AMPARs is also macroscopically non-decaying, but potentiated by cyclothiazide (Weston *et al.* 2006), which is thought to block desensitization. This observation is surprising because crosslinking the LBD dimer would be expected to fully eliminate desensitization. Given the results presented in this study, however, we predict that this AMPAR mutation would have similar single-channel responses as those reported here. Interestingly, crosslinking the NMDA receptor dimer interface at equivalent residues does not affect receptor desensitization but instead regulates open-channel probability (Borschel *et al.* 2011). Since we have observed that the same manipulation on KARs regulates unitary conductance, we propose that the LBD dimer interface may have adapted to fulfil different tasks as distinct iGluR subfamilies emerged during evolution.

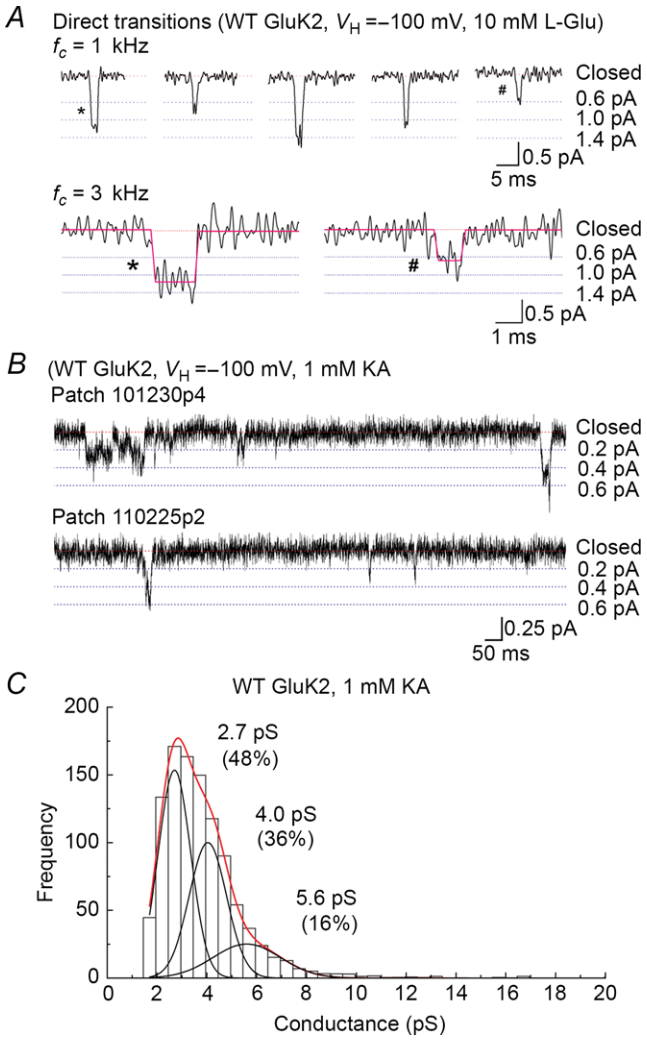

Figure 6. Single-channel events elicited by L-Glu and KA
A, single-channel events evoked at a holding potential (V_H) of −100 mV for wild-type (WT) GluK2 shows direct transitions into the large amplitude levels (>0.6 pA) during continuous activation by 10 mM L-Glu. Offline filtering (f_c) at 3 kHz produced similar idealized records. *B*, typical single-channel events elicited from WT GluK2 in the continuous presence of 1 mM KA. *C*, frequency distribution of single event amplitudes from three patches was fitted with the sum of three Gaussian components.

Working towards a new mechanism of kainate receptor gating

The molecular basis of KAR gating has been a matter of debate. In particular, it remains to be established how KAR stimulation by agonist leads to electrophysiological

responses that exhibit both a large, transient peak and much smaller sustained or steady-state component. Two explanations have been proposed. Most studies have explained the rapid decay from the peak of KAR responses by the onset of receptor desensitization (e.g. Heckmann *et al.* 1996; Bowie *et al.* 1998; Barberis *et al.* 2008) using models based on pioneering work at nicotinic acetylcholine receptors (Del Castillo & Katz, 1957) and more recent studies of AMPARs (Robert *et al.* 2005). In the context of the present study, a key signature of these models is that the open states that constitute the peak and steady-state responses are the same. Thus, differences in peak and steady-state response amplitude are due entirely to the onset of desensitization. The problem with these models when applied to KARs is that they cannot fully explain several key aspects of gating such as (i) the multi-exponential nature of KAR desensitization (Bowie & Lange, 2002), (ii) the selective effect of concanavalin-A on equilibrium but not peak responses (Bowie *et al.* 2003) and (iii) the functional profile of full and partial KAR agonists (Maclean *et al.* 2011).

An alternative viewpoint is that the amplitude of the unitary conductance state(s) that gives rise to the peak response is significantly larger than the unitary conductance state(s) that constitutes the steady-state response (Bowie & Lange, 2002; Bowie *et al.* 2003; Maclean *et al.* 2011). Here, desensitization still plays a role but the decline in response amplitude is also due to the relaxation into lower conductance states. Importantly, this model is able to explain the many properties of KARs mentioned above, as well as data presented in this study, and is also consistent with a recent study showing that transient activation of GluK2 receptors gates channels with a large open state of about 27 pS (Zhang *et al.* 2009).

However, more complex mechanisms may be at play. For example, KAR activation need not necessarily begin from the same starting point as would occur in the sequential model of gating (Bowie & Lange, 2002). Instead, agonist binding could lead to one of two possible activated states with the first having a large unitary conductance as described by others (Zhang *et al.* 2009) and the second having the low conductance described in the present study. Clearly much remains to be resolved, suggesting that future work on KAR gating will not only provide better insight into their functional properties but also how they relate to structure.

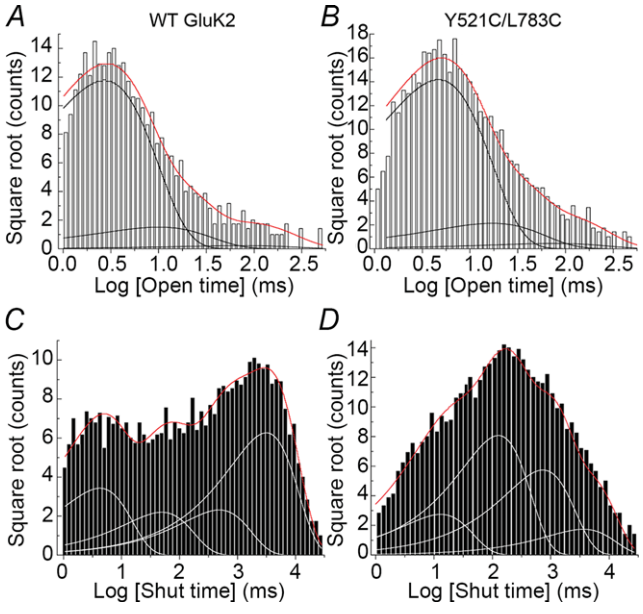

Figure 7. Kinetic properties of single-channel events of wild-type and Y521C/L783C GluK2 receptors
Open time (*A* and *B*) and closed time (*C* and *D*) distributions for wild-type (WT) and Y521C/L783C GluK2 receptors were compiled from time course fitted data offline filtered at 1 kHz. Resolution was set to 0.9 ms for open times and 0.8 ms for shut times. Binned data were fitted with the sum of three (open times) or four (shut times) exponential components (see Table 1 for measured times).

References

Aldrich RW, Corey DP & Stevens CF (1983). A reinterpretation of mammalian sodium channel gating based on single channel recording. *Nature* **306**, 436–441.

Ascher P, Bregestovski P & Nowak L (1988). *N*-methyl-D-aspartate-activated channels of mouse central neurones in magnesium-free solutions. *J Physiol* **399**, 207–226.

Barberis A, Sachidhanandam S & Mulle C (2008). GluR6/KA2 kainate receptors mediate slow-deactivating currents. *J Neurosci* **28**, 6402–6406.

Barry PH, Schofield PR & Moorhouse AJ (1999). Glycine receptors: what gets in and why? *Clin Exp Pharmacol Physiol* **26**, 935–936.

Borschel WF, Murthy SE, Kasperek EM & Popescu GK (2011). NMDA receptor activation requires remodelling of intersubunit contacts within ligand-binding heterodimers. *Nat Commun* **2**, 498.

Bowie D (2002). External anions and cations distinguish between AMPA and kainate receptor gating mechanisms. *J Physiol* **539**, 725–733.

Bowie D, Garcia EP, Marshall J, Traynelis SF & Lange GD (2003). Allosteric regulation and spatial distribution of kainate receptors bound to ancillary proteins. *J Physiol* **547**, 373–385.

Bowie D & Lange GD (2002). Functional stoichiometry of glutamate receptor desensitization. *J Neurosci* **22**, 3392–3403.

Bowie D, Lange GD & Mayer ML (1998). Activity-dependent modulation of glutamate receptors by polyamines. *J Neurosci* **18**, 8175–8185.

Chaudhry C, Weston MC, Schuck P, Rosenmund C & Mayer ML (2009). Stability of ligand-binding domain dimer assembly controls kainate receptor desensitization. *EMBO J* **28**, 1518–1530.

Colquhoun D. (1994). Practical analysis of single channel records. In Ogden DC 2nd edn, 101–139. Cambridge, UK, The Company of Biologists Limited. The Plymouth Workshop Handbook: Microelectrode Techniques.

Colquhoun D & Ogden DC (1988). Activation of ion channels in the frog end-plate by high concentrations of acetylcholine. *J Physiol* **395**, 131–159.

Colquhoun D & Sigworth FJ (1995). Fitting and statistical analysis of single channel records. In *Single-Channel Recording*, eds Sakmann B & Neher E, pp. 483–588. Plenum Press, New York.

Del Castillo J. & Katz B (1957). Interaction at end-plate receptors between different choline derivatives. *Proc R Soc Lond B Biol Sci* **146**, 369–381.

Fay AM, Corbeil CR, Brown P, Moitessier N & Bowie D (2009). Functional characterization and in silico docking of full and partial GluK2 kainate receptor agonists. *Mol Pharmacol* **75**, 1096–1107.

Fleck MW, Cornell E & Mah SJ (2003). Amino-acid residues involved in glutamate receptor 6 kainate receptor gating and desensitization. *J Neurosci* **23**, 1219–1227.

Fox JA (1987). Ion channel subconductance states. *J Membr Biol* **97**, 1–8.

Hamill OP, Bormann J & Sakmann B (1983). Activation of multiple-conductance state chloride channels in spinal neurones by glycine and GABA. *Nature* **305**, 805–808.

Heckmann M, Bufler J, Franke C & Dudel J (1996). Kinetics of homomeric GluR6 glutamate receptor channels. *Biophys J* **71**, 1743–1750.

Jin R, Clark S, Weeks AM, Dudman JT, Gouaux E & Partin KM (2005). Mechanism of positive allosteric modulators acting on AMPA receptors. *J Neurosci* **25**, 9027–9036.

Katz B & Thesleff S (1957). A study of the desensitization produced by acetylcholine at the motor end-plate. *J Physiol* **138**, 63–80.

Liu B, Yao J, Wang Y, Li H & Qin F (2009). Proton inhibition of unitary currents of vanilloid receptors. *J Gen Physiol* **134**, 243–258.

McAllister AK & Stevens CF (2000). Nonsaturation of AMPA and NMDA receptors at hippocampal synapses. *Proc Natl Acad Sci U S A* **97**, 6173–6178.

Maclean DM, Wong AY, Fay AM & Bowie D (2011). Cations but not anions regulate the responsiveness of kainate receptors. *J Neurosci* **31**, 2136–2144.

Mulle C, Vidal C, Benoit P & Changeux JP (1991). Existence of different subtypes of nicotinic acetylcholine receptors in the rat habenulo-interpeduncular system. *J Neurosci* **11**, 2588–2597.

Nayeem N, Zhang Y, Schweppe DK, Madden DR & Green T (2009). A nondesensitizing kainate receptor point mutant. *Mol Pharmacol* **76**, 534–542.

Neher E & Stevens CF (1977). Conductance fluctuations and ionic pores in membranes. *Annu Rev Biophys Bioeng* **6**, 345–381.

Partin KM, Fleck MW & Mayer ML (1996). AMPA receptor flip/flop mutants affecting deactivation, desensitization, and modulation by cyclothiazide, aniracetam, and thiocyanate. *J Neurosci* **16**, 6634–6647.

Priel A, Selak S, Lerma J & Stern-Bach Y (2006). Block of kainate receptor desensitization uncovers a key trafficking checkpoint. *Neuron* **52**, 1037–1046.

Robert A, Armstrong N, Gouaux JE & Howe JR (2005). AMPA receptor binding cleft mutations that alter affinity, efficacy, and recovery from desensitization. *J Neurosci* **25**, 3752–3762.

Root MJ & MacKinnon R (1993). Identification of an external divalent cation-binding site in the pore of a cGMP-activated channel. *Neuron* **11**, 459–466.

Rosenmund C, Stern-Bach Y & Stevens CF (1998). The tetrameric structure of a glutamate receptor channel. *Science* **280**, 1596–1599.

Ruiz ML & Karpen JW (1997). Single cyclic nucleotide-gated channels locked in different ligand-bound states. *Nature* **389**, 389–392.

Smith TC & Howe JR (2000). Concentration-dependent substate behaviour of native AMPA receptors. *Nat Neurosci* **3**, 992–997.

Stern-Bach Y, Russo S, Neuman M & Rosenmund C (1998). A point mutation in the glutamate binding site blocks desensitization of AMPA receptors. *Neuron* **21**, 907–918.

Sun Y, Olson R, Horning M, Armstrong N, Mayer M & Gouaux E (2002). Mechanism of glutamate receptor desensitization. *Nature* **417**, 245–253.

Swanson GT, Feldmeyer D, Kaneda M & Cull-Candy SG (1996). Effect of RNA editing and subunit co-assembly single-channel properties of recombinant kainate receptors. *J Physiol* **492**, 129–142.

Swanson GT, Green T, Sakai R, Contractor A, Che W, Kamiya H & Heinemann SF (2002). Differential activation of individual subunits in heteromeric kainate receptors. *Neuron* **34**, 589–598.

Weston MC, Schuck P, Ghosal A, Rosenmund C & Mayer ML (2006). Conformational restriction blocks glutamate receptor desensitization. *Nat Struct Mol Biol* **13**, 1120–1127.

Zhang W, St-Gelais F, Grabner CP, Trinidad JC, Sumioka A, Morimoto-Tomita M, Kim KS, Straub C, Burlingame AL, Howe JR & Tomita S (2009). A transmembrane accessory subunit that modulates kainate-type glutamate receptors. *Neuron* **61**, 385–396.

Zhang Y, Nayeem N, Nanao MH & Green T (2006). Interface interactions modulating desensitization of the kainate-selective ionotropic glutamate receptor subunit GluR6. *J Neurosci* **26**, 10033–10042.

Additional information

Competing interests

None.

Author contributions

D.B., B.A.D., E.D.A. and M.R.P.A. designed the experiments and wrote and edited the manuscript. B.A.D., E.D.A. and M.V.A. performed the experiments and analysed the data. All authors approved this manuscript.

Funding

This work was supported by operating grants from the Canadian Institutes of Health Research (CIHR) to D.B. B.A.D. was supported by a Chemical Biology CIHR postdoctoral award, E.D.A. by a graduate student fellowship from the Natural Sciences and Engineering Research Council of Canada (NSERC), M.R.P.A. by a CIHR Best & Banting doctoral award and M.V.A. by a Max Stern Fellowship and a McGill Faculty of Medicine award. D.B. is the recipient of a Canada Research Chair award.

Acknowledgements

We wish to thank Dr Anthony Auerbach for discussions on desensitization and Brent Dawe and Patricia Brown for insightful comments on the manuscript.